2010 IEEE Energy Conversion Congress and Exposition, pp. 4376-4383, Sept. 2010.

Inductor Design Methods with Low-permeability RF Core Materials

Yehui Han
University of Wisconsin - Madison
2559C Engineering Hall, 1415 Engineering Drive
Madison, WI 53706, USA
Email: yehui@engr.wisc.edu

David J. Perreault
Laboratory for Electromagnetic and Electronic Systems
Massachusetts Institute of Technology, Room 10-171
Cambridge, Massachusetts 02139, USA
Email: djperrea@mit.edu

***Abstract*—This paper presents a design procedure for inductors based on low-permeability magnetic materials for use in very high frequency (VHF) power conversion. The proposed procedure offers an easy and fast way to compare different magnetic materials based on Steinmetz parameters and quickly select the best among them, estimate the achievable inductor quality factor and size, and finally design the inductor. Geometry optimization of magnetic-core inductors is also investigated. The proposed design procedure and methods are verified by experiments.**

I. Background

There is a growing interest in switched-mode power electronics capable of efficient operation at very high switching frequencies (e.g., 10-100 MHz) [1]. These designs utilize magnetic components operating at high frequencies, and often under large flux swings. These magnetic components should have a high quality factor to achieve high efficiency power conversion. Unfortunately, most high-permeability magnetic materials exhibit unacceptably high losses at frequencies above a few megahertz. There are some low-permeability materials (e.g., relative permeabilities in the range of 4-40) that can be used effectively at moderate flux swings at frequencies up to many tens of megahertz [2]. However, working with such low-permeability materials - and the ungapped core structures they are typically available in - presents somewhat different constraints and challenges than with typical high-permeability low-frequency materials [3]. Because of VHF operation and low-permeability characteristics of such materials, the operating flux density is limited by core loss rather than saturation, and a gap is not necessary to prevent the core from saturating in many applications. Without a gap, the core loss begins to dominate the total loss and copper loss can be ignored in many cases. The performance of a VHF magnetic-core inductor thus depends heavily on the loss characteristics of the magnetic material. Moreover, there appears to be a lack of good design procedures for a selecting among low-permeability magnetic materials and available core sizes.

In this paper, we propose a design procedure for inductors using low-permeability magnetic materials. This method is based on knowledge of the material loss characteristics, such as collected in [2], and is particularly suited for VHF inductor designs. With methods used in this procedure, different magnetic materials are compared fairly and conveniently, and both the achievable quality factor and size of a magnetic-core inductor can be evaluated before the final design.

Section II of the paper introduces the inductor design considerations and questions to be addressed. Section III illustrates the inductor design procedure and methods employed in it. Section IV shows some experimental results to verify the design procedure. Section V concludes the paper. In Appendix, we check an important assumption behind our methods as well as investigate geometry optimization problems of magnetic-core inductors.

II. Inductor Design Considerations and Questions

In our paper, we only consider inductor designs under a limited set of conditions in order to make the problem tractable. Nevertheless, these conditions are both very reasonable and practical for inductors at very high frequencies. The limited conditions we address are as follows:

1) Use of ungapped cores made of low-permeability materials.
2) Single-layer, foil wound designs in the skin depth limit on toroidal core shapes. A toroidal inductor design keeps most of flux inside the core, thus reducing EMI/EMC problems. A foil winding design can further reduce the copper loss compared to a wire-wound one [4].
3) Design based on knowledge of Steinmetz parameters for materials of interest. Such parameters are often not published or readily available for these materials, but can be obtained using methods such as that of [2].
4) Design assuming sinusoidal excitation at one frequency. In VHF resonant inverters or converters, inductors often have approximately sinusoidal current at a single frequency. Note that consideration of variable frequency operation, dc currents, and multiple frequency components greatly increases complexity.

Fig. 1 shows an inductor design under the above conditions.

Given a selection of available cores in different low-permeability materials, and a design specification including inductance L, current amplitude I_{pk}, frequency f_s, we answer three important questions about design of VHF inductors under the above conditions:

1) Which magnetic material from an available set will yield maximum quality factor Q_L for a given size?
2) Given the ability to continuously scale core size, what material will yield the smallest size for a given quality factor Q_L?
3) For an achievable quality factor Q_L and inductor size, how should we design the inductor with the selected best magnetic material to meet design specifications?

We answer these questions in the next section.

III. Inductor Design Procedure and Methods

A. Inductor Design Procedure

Fig. 2 illustrates the proposed design procedure. First, select design specifications from the system requirements. Second, select the best magnetic material from a set of low-permeability materials with known Steinmetz parameters. In the third and fourth steps, we estimate the achievable quality factor Q_L and size of the inductor with the best available material. If the results are satisfactory, we design the inductor. If not, it means the design requirements can't be satisfied even with the best available magnetic material, and one must revise the inductor design requirements. A key feature of this design procedure is that magnetic materials are compared first and the best material is selected before completing any individual design, greatly reducing design time and effort. Some important information such as the maximum quality factor Q_L, and the smallest possible size can be acquired before the final design. By this procedure, we design an inductor only with one size and one material instead of investigating thousands of combinations to meet the design specifications.

(1) to (3) are used often in our design procedure. In VHF power conversion, ac losses (conductor/copper and core losses) usually dominate and we thus ignore dc losses (conductor loss) here. In (1) and (2), we use the quality factor Q_L to evaluate the ac losses of an inductor at a single frequency. R_{ac} is the equivalent total ac resistance of a magnetic-core inductor including copper loss and core loss, R_{cu} is the equivalent resistance owing to copper loss, and R_{co} is an equivalent resistance owing to core loss. The Steinmetz equation is an empirical means to estimate loss characteristics of magnetic materials. It has many extensions, but we only consider the formulation for sinusoidal drive at a single frequency here. In (3), B_{pk} is the peak amplitude of average (sinusoidal) flux density inside the material and P_V is power loss per unit core volume [1]. K and β are called Steinmetz parameters. K and β have been calculated for several commercial low-permeability rf magnetic materials in [2].

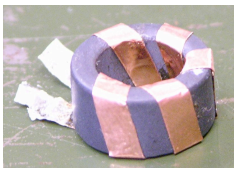

Fig. 1. An example of an inductor fabricated from copper foil on a commercial magnetic core M3-998 from National Magnetics Group.

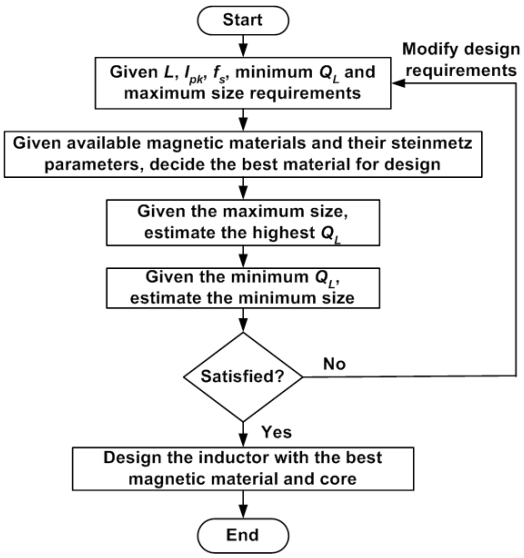

Fig. 2. Inductor design procedure

$$Q_L = \frac{\omega L}{R_{ac}} \tag{1}$$

$$R_{ac} = R_{cu} + R_{co} \tag{2}$$

$$P_V = K B_{pk}^{\beta} \tag{3}$$

B. Method to Select Among Magnetic Materials

In the second step, we begin with a coreless inductor to make a comparison among different design options (including magnetic materials) for a given L, I_{pk}, f_s, minimum Q_L and maximum size limitation. Ignoring the inductance of single-turn loop, the number of turns N_{air} for a coreless inductor can be calculated from (4) [4]:

$$N_{air} \approx \sqrt{\frac{2\pi L}{h\mu_0 \ln\left(\frac{d_o}{d_i}\right)}} \tag{4}$$

d_o, d_i and h are the outside diameter, inside diameter and height of the coreless inductor. Its average flux density B_{pk-air} inside the core is calculated by (5):

$$B_{pk-air} = \frac{\mu_0 N_{air} I_{pk}}{0.5\pi(d_i + d_o)} \tag{5}$$

Likewise, the number of turns N and average flux density B_{pk} of a magnetic-core inductor are calculated by (6) and (7):

$$N \approx \sqrt{\frac{2\pi L}{h\mu_0\mu_r \ln\left(\frac{d_o}{d_i}\right)}} \tag{6}$$

$$B_{pk} = \frac{\mu_0\mu_r N I_{pk}}{0.5\pi(d_i + d_o)} = \mu_r^{0.5} B_{pk-air} \tag{7}$$

[1] Use of average flux density in the core simplifies the calculations. For typical core sizes, this approximation can be shown to be well justified [5].

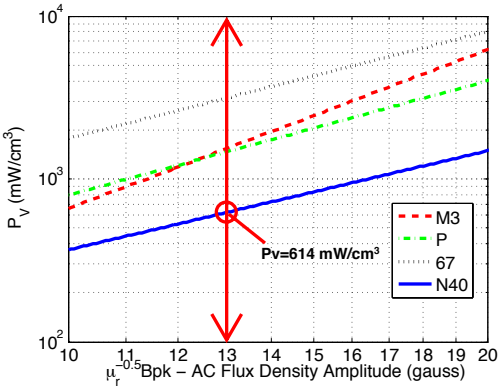

Fig. 3. Inductor design example ($d_o = 12.7$ mm, $d_i = 6.3$ mm, $h = 6.3$ mm, $L = 200$ nH, $I_{pk} = 2$ A, $f_s = 30$ MHz and $B_{pk-air} = 13$ G).

For a given L and specified dimensions in (7), average flux density B_{pk} inside the core may be different for each magnetic material, which is one of the reasons we can't compare their loss characteristics for different magnetic materials directly at the same flux density level. However, we propose here a method by which direct comparisons can be made: B_{pk} of each magnetic material can be normalized to the coreless inductor flux density B_{pk-air} by its relative permeability μ_r. For a given design specification, all magnetic materials will have the same normalized flux density, which is equal to $\mu_r^{-0.5}B_{pk}$. Given a set of Steinmetz parameters, we can draw the curves of P_V vs. $\mu_r^{-0.5}B_{pk}$ for all available magnetic materials. We compare P_V of these materials at $\mu_r^{-0.5}B_{pk} = B_{pk-air}$ and decide which material has the smallest core loss for the given design specification.

An example is shown in Fig. 3, in which we consider a design of a magnetic-core inductor at $I_{pk} = 2$ A and $f_s = 30$ MHz with $L = 200$ nH and maximum size $d_o = 12.7$ mm, $d_i = 6.3$ mm and $h = 6.3$ mm. Beginning with a coreless inductor, we calculate $B_{pk-air} = 13$ G from (4) and (5). Using data from [2], loss curves of P_V vs. $\mu_r^{0.5}B_{pk}$ are plotted for the materials N40, P, M3 and 67 [2]. We compare their P_V at B_{pk-air} and find that N40 material has the smallest core loss (614 mw/cm^3). If we ignore the copper loss, the magnetic-core inductor with N40 material will achieve the highest Q_L for given design specifications. We can also observe in Fig. 3 that N40 is better than the other magnetic materials and 67 is worse than the others over a wide range of flux density. This will help us to design a magnetic-core inductor if its current operating level is unknown or very wide.

We still don't know if the magnetic-core inductor with the best material is better than a coreless inductor of the same size. There is no core loss and Steinmetz parameter for a coreless inductor. But we can still compare its copper loss to core losses of other magnetic materials on the same graph.

[2] -17 material in [2] has a very low relative permeability and low core loss characteristics. Compared to its core loss, the copper loss of -17 material can't be ignored. As a special case, -17 is not considered here. However, the methods introduced in this paper can still be applied for -17 material with special considerations of its copper loss.

To accommodate the coreless design, we define P_{V-air} at B_{pk-air} as the power loss per unit volume for a coreless inductor and calculate it by (8):

$$P_{V-air} = \frac{R_{cu-air}}{2V} I_{pk}^2 \tag{8}$$

R_{cu-air} is the copper resistance of a coreless inductor. R_{cu-air} (or the copper resistance of a magnetic-core inductor R_{cu}) depends heavily on a coreless or magnetic-core inductor winding design pattern. One could find the ac resistance of a coreless inductor by constructing and measuring it or simulating it using computational techniques. Alternatively, the resistance can be estimated for different design variants:

1) In [2], the windings are made of an equal-width foil-like conductor, and $R_{cu-single-turn}$ is the ac copper resistance of a single turn inductor:

$$\begin{aligned} R_{cu} &= N^2 R_{cu-single-turn} \\ &\approx N^2 \frac{\rho_{cu}}{\pi \delta_{cu}} \left(\frac{2h}{d_i} + \frac{d_o}{d_i} - 1 \right) \end{aligned} \tag{9}$$

2) In [2], R_{cu} can alternatively be estimated from the foil width, length and skin depth:

$$R_{cu} \approx \frac{\rho_{cu} l_{cu}}{\delta_{cu} w_{cu}} \tag{10}$$

3) In [4], the windings are made of foil-like conductor tapered to conform to the shape of the toroid:

$$\begin{aligned} R_{cu} &= N^2 R_{cu-single-turn} \\ &\approx N^2 \frac{\rho_{cu}}{\pi \delta_{cu}} \left(\frac{h}{d_i} + \frac{h}{d_o} + 2 \ln \frac{d_o}{d_i} \right) \end{aligned} \tag{11}$$

For example, the loss characteristics of a coreless inductor estimated by (9) is included in Fig. 4 . We can see N40 is the only magnetic material which has lower loss than the coreless inductor. Thus the magnetic-core inductor built with N40 may have a higher quality factor Q_L than the coreless inductor. The magnetic-core inductor built by other materials (e.g. M3, P and 67) will not be better than the coreless inductor and not be considered in the following steps. Here, we can see that this comparison lets us exclude most of available magnetic materials in the pool from the design, saving time and effort.

From previous measurements in [2], the core loss (R_{co}) usually dominates the total loss of an ungapped VHF magnetic-core inductor. However, this statement should be checked to make sure that it is still correct for an individual design. By a similar method, we can define the copper loss per unit volume P_{V-cu} of a magnetic-core inductor and mark it on the graph of P_V vs. $\mu_r^{0.5}B_{pk}$. From (4) and (6),

$$N = \mu_r^{-0.5} N_{air} \tag{12}$$

$$R_{cu} = N^2 R_{cu-single-turn} = \mu_r^{-1} R_{cu-air} \tag{13}$$

$$P_{V-cu} = \frac{R_{cu}}{2V} I_{pk}^2 = \frac{\mu_r^{-1} R_{cu-air}}{2V} I_{pk}^2 = \mu_r^{-1} P_{V-air} \tag{14}$$

P_{V-air} can be calculated from (8). The copper loss characteristic of a magnetic-core inductor for the example specifications

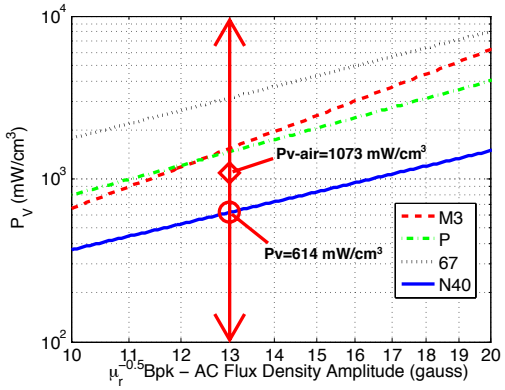

Fig. 4. Inductor design example including the power loss characteristic of a coreless inductor ($d_o = 12.7$ mm, $d_i = 6.3$ mm, $h = 6.3$ mm, $L = 200$ nH, $I_{pk} = 2$ A, $f_s = 30$ MHz and $B_{pk-air} = 13$ G).

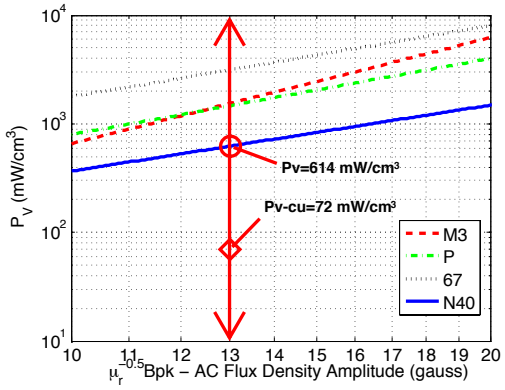

Fig. 5. Inductor design example including the copper loss characteristic of a magnetic-core inductor ($d_o = 12.7$ mm, $d_i = 6.3$ mm, $h = 6.3$ mm, $L = 200$ nH, $I_{pk} = 2$ A, $f_s = 30$ MHz and $B_{pk-air} = 13$ G).

built in N40 magnetic material is marked in Fig. 5. In this example, the copper loss of the magnetic-core inductor is much smaller than its core loss (an order of magnitude or more [3]).

C. Q_L Estimation with Given Maximum Inductor Size

In the third step, if we ignore the copper loss comparing to the core loss of the magnetic-core inductor, the quality factor Q_L can be estimated by (15) and (16):

$$R_{co} \approx \frac{Total\ Core\ Loss}{0.5I_{pk}^2} = \frac{P_V V}{0.5I_{pk}^2} \tag{15}$$

$$Q_L \approx \frac{\omega L}{R_{co}} = \omega L \frac{0.5I_{pk}^2}{P_V V} \tag{16}$$

E.g., for the magnetic-core inductor built in N40, $P_V = 700$ mW/cm^3 at $B_{pk-air} = 13$ G, and $Q_L \approx 198$ by (16). In this example $R_{co} \approx 0.19$ and $R_{cu} \approx 0.03$, where $R_{co} \gg R_{cu}$. Q_L can also be estimated by (2), in which copper loss is included, and $Q_L \approx 171$ by (2).

[3]We note that the simple copper loss calculations of (9) in a cored inductor design may have up to 30% error [2], but this degree of accuracy is sufficient for our present purposes.

D. Size Estimation with Given Minimum Q_L

In this subsection, we illustrate the third step in our inductor design procedure. Because the method introduced in this subsection is not as simple and direct as the method in Section III-B, we begin this subsection with a general description of the method. Then we derive equations needed in our method for inductor size estimation. As we have done in Section III-B, step by step design examples are given to aid understanding of the method.

We again begin with a coreless inductor design, calculate its size and compare the size of a magnetic-core inductor with it. In our method, we define the scaling factor λ as the dimension ratio of a magnetic-core inductor and the coreless inductor for given L, Q_L, f_s and I_{pk}, and we assume that the relative ratio of the 3 dimensions is kept constant during the scaling. Thus, we scale each dimension (x, y, z) describing the shape of the coreless inductor by a factor λ to get the corresponding dimension of a magnetic-core inductor: the coreless inductor thus has $\lambda = 1$, and the magnetic-core inductor with the minimum λ has the smallest size.

Our method has four main steps:

1) Given L, I_{pk}, f_s and minimum required Q_L, design a coreless inductor and get its dimension parameters d_o, d_i, h.
2) Calculate B_{pk-air} of the coreless inductor, compare its P_{V-air} to P_V of other magnetic materials at B_{pk-air} on the graph of P_V vs. $\mu_r^{-0.5}B_{pk}$ and decide the possible best materials for the inductor design.
3) Calculate the scaling factor λ for the possible best materials.
4) Check the flux density B'_{pk}, core loss $P_{V'}$, and copper loss $P_{V'-cu}$ of the magnetic-core inductor after scaling on the graph of P_V vs. $\mu_r^{-0.5}B_{pk}$.

1) Step I, Calculate Coreless Design: From (4), the quality factor Q_L of a coreless inductor can be calculated by (17):

$$Q_L = \frac{\omega L}{R_{cu-air}} = \frac{\mu_0 f_s}{R_{cu-single-turn}} h \ln\left(\frac{d_o}{d_i}\right) \tag{17}$$

$R_{cu-single-turn}$ can be estimated by (9) or (11).

If we assume $d_i = 0.5d_o$, we can solve the dimension parameters d_o, d_i, h of a coreless inductor from (9)/(11), and (17) for given f_s and Q_L. In Appendix A, we show that this assumption is very reasonable because letting $d_i = 0.5d_o$ yields an inductor with nearly optimum Q_L and thus the smallest size.

2) Step II, Evaluate Magnetic Materials: After calculating the dimensions of the coreless inductor, its B_{pk-air} and P_{V-air} can be calculated by (5) and (8). P_V at B_{pk-air} of all the magnetic materials can be found from the graph of P_V vs. $\mu_r^{-0.5}B_{pk}$. For example, we consider the design of a coreless inductor with $L = 200$ nH, $I_{pk} = 2$ A, $f_s = 30$ MHz, and $Q_L = 116$. We define this coreless inductor as having $\lambda = 1$. Its dimensions are $d_o = 12.7$ mm, $d_i = 6.3$ mm and $h = 6.3$ mm. The question we seek to answer is: if we build a magnetic-core inductor with magnetic materials, how small

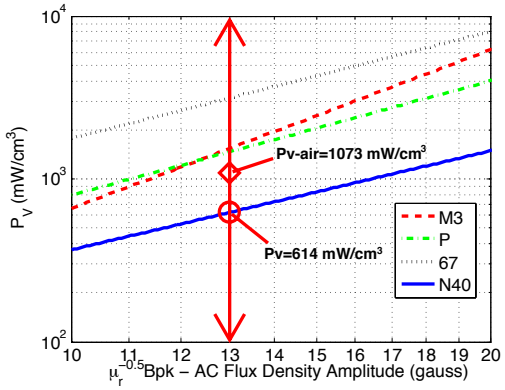

Fig. 6. Loss plots of inductor design scaling example ($d_o = 12.7$ mm, $d_i = 6.3$ mm, $h = 6.3$ mm, $L = 200$ nH, $I_{pk} = 2$ A, $f_s = 30$ MHz and $B_{pk-air} = 13$ G).

it could be while achieving specified Q_L. We firstly calculate $B_{pk-air} = 13$ G and $P_{V-air} = 1073$ mW/cm^3 and then find P_V for each magnetic material in Fig. 7. N40 is the only magnetic material which has P_V smaller than P_{V-air}, thus the magnetic-core inductor made in N40 is the only possible design with the size smaller than the coreless inductor ($\lambda < 1$). Magnetic-core inductors made by other materials will have larger sizes than the coreless inductor and are not considered here. This conclusion is further proved in (26). Just as in Section III-B, we can see here our method in this subsection again helps us to exclude many available magnetic materials in the pool from the complicated problem of inductor size scaling.

3) Step III, Scaling: Here we introduce how to perform the scaling. Before beginning derivation, we define the following parameters:

1) V, d_o, d_i, h, N, B_{pk}, P_V, P_{V-cu}, R_{co} and R_{cu} are the volume, outside diameter, inside diameter, height, number of turns, average peak ac flux density, core loss density, copper loss density, equivalent core resistance, and copper resistance of a magnetic-core inductor before scaling - i.e., having the same size as the coreless inductor ($\lambda = 1$).
2) V', d'_o, d'_i, h', N', B'_{pk}, P'_V, $P_{V'-cu}$, R'_{co} and R'_{cu} are the same definitions of the magnetic-core inductor after scaling.
3) V, d_o, d_i, h, N_{air}, B_{pk-air}, P_{V-air} and R_{cu-air} are the similiar definitions of the coreless inductor before scaling ($\lambda = 1$)

From the definition above,

$$\lambda = \frac{d'_o}{d_o} = \frac{d'_i}{d_i} = \frac{h'}{h} \tag{18}$$

$$V' = \lambda^3 V \tag{19}$$

Thus: similar to (6),

$$N' = \sqrt{\frac{2\pi L}{\lambda h \mu_0 \mu_r \ln\left(\frac{\lambda d_o}{\lambda d_i}\right)}} = \lambda^{-0.5} N \tag{20}$$

Similar to (7) and from (20),

$$B'_{pk} = \frac{\mu_0 \mu_r N' I_{pk}}{0.5\pi(d'_i + d'_o)} = \lambda^{-1.5} B_{pk} \tag{21}$$

$$P_{V'} = K B'^{\beta}_{pk} = \lambda^{-1.5\beta} P_V \tag{22}$$

From (9) and (11), we observe that $R_{cu-single-turn}$ is constant during scaling. This is because the effective conductor thickness is the skin depth (invariant to scaling). This results in constant "ohms per square", making the total single-turn resistance invariant to scaling. From (12) and (20),

$$R'_{cu} = N'^2 R_{cu-single-turn} = \lambda^{-1} \mu_r^{-1} R_{cu-air} \tag{23}$$

Similar to (14), and from (19) and (23):

$$P_{V'-cu} = \frac{R'_{cu}}{2V'} I^2_{pk} = \lambda^{-4} \mu_r^{-1} P_{V-air} \tag{24}$$

For constant Q_L, the total loss is the same for both the coreless inductor and the magnetic-core inductor, thus from (19), (22) and (24):

$$P_{V'} V' + P_{V'-cu} V' = P_{V-air} V \tag{25}$$

$$\lambda^{3-1.5\beta} \frac{P_V}{P_{V-air}} + \lambda^{-1} \mu_r^{-1} = 1 \tag{26}$$

The scaling factor λ can be calculated by (26), if we know P_V, relative permeability μ_r, and Steinmetz parameter β of the magnetic material, and P_{V-air} of the coreless inductor. Because of the usual case for Steinmetz parameters, P_V should be smaller than P_{V-air} to get $\lambda < 1$ from (26). This explains why we don't have to consider magnetic materials which have P_V larger than P_{V-air}. (26) is the key equation for calculating achievable design scaling at constant Q_L through the use of an ungapped magnetic core.

Let's continue our example shown in Fig. 7. For N40 material, $P_V = 614$ mw/cm^3 at $B_{pk-air} = 13$ G, $\beta = 2.02$ at 30 MHz and $\mu_r = 15$, the scaling factor $\lambda = 0.17$ by (26).

4) Step IV, Check Design Assumptions: As a last step, we check the flux density B'_{pk}, core loss P'_V, and copper loss $P_{V'-cu}$ of the inductor after scaling on the graph of P_V vs. $\mu_r^{-0.5} B_{pk}$. From (7) and (21):

$$\frac{B'_{pk}}{\sqrt{\mu_r}} = \lambda^{-1.5} B_{pk-air} \tag{27}$$

In the example, $P'_V = 1.3 \times 10^5$ mW/cm^3 by (22) and $P'_{V-cu} = 8.6 \times 10^4$ mW/cm^3 by (24) are shown in Fig. 7. We can still see that the core loss dominates the total loss. With completion of this last step, we now have an inductor geometry and scaling that achieves the smallest size at the required Q_L.

5) Inductor Scaling with Multi-choice of Magnetic Materials: Here we gives an example of solution if there are more than one possible best material which can be used to build a cored inductor having smaller size than the coreless inductor and thus $\lambda < 1$.

We consider the design of a coreless inductor with $L = 200$ nH, $I_{pk} = 0.5$ A, $f_s = 30$ MHz, and $Q_L = 116$. We design a coreless inductor which has $\lambda = 1$ and dimensions

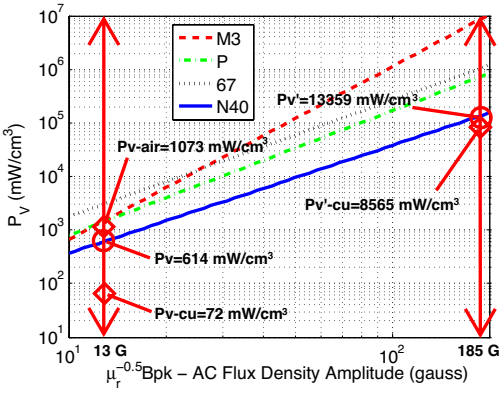

Fig. 7. The magnetic-core inductor after scaling design

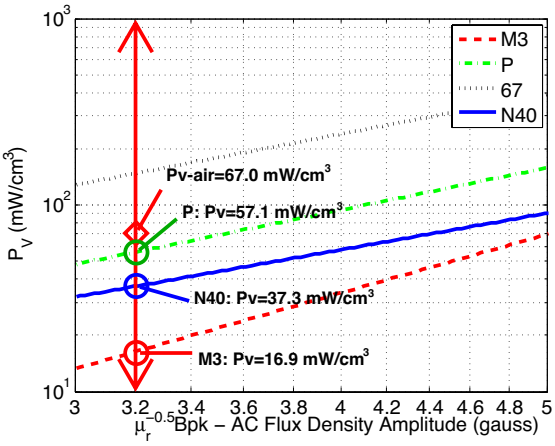

Fig. 8. Loss plots of inductor design scaling example ($d_o = 12.7$ mm, $d_i = 6.3$ mm, $h = 6.3$ mm, $L = 200$ nH, $I_{pk} = 0.5$ A, $f_s = 30$ MHz and $B_{pk-air} = 3.2$ G).

of $d_o = 12.7$ mm, $d_i = 6.3$ mm and $h = 6.3$ mm. We firstly calculate $B_{pk-air} = 3.2$ G and $P_{V-air} = 67$ mW/cm^3 and then find P_V for each magnetic material in Fig. 8. P, M3 and N40 are magnetic materials which have P_V smaller than P_{V-air}, thus magnetic-core inductors made with these three materials may possibly be smaller than the coreless inductor ($\lambda < 1$). P material has a larger core loss P_V at B_{pk-air} as well as a larger slope ($= \beta$) of the loss curve than N40 material, so we can conclude that the magnetic-core inductor built with P material should have a higher loss and lower Q_L than the same size magnetic-core inductor built with N40 material. However, we can't immediately determine which of M3 and N40 materials is better: M3 has a lower P_V but a higher slope of the loss curve than N40. We thus consider both M3 and N40 as possible best materials and calculate their scaling factor λ by (26). We list the calculation results in Table I which also includes P material to confirm our conclusion. From Table I, we can see that the magnetic-core inductor built with N40 still has the smallest scaling factor, and represents the best design choice.

We check the flux density B'_{pk}, core loss P'_V, and copper

TABLE I

COMPARISON OF SCALING FACTOR λ AMONG MAGNETIC-CORE INDUCTORS BUILT WITH P, M3 AND N40 MATERIALS.

Material	P	M3	N40
P_V (mW/cm^3)	57.1	16.9	37.3
μ_r	40	12	15
β	2.33	3.24	2.02
λ by (26)	0.77	0.52	0.16

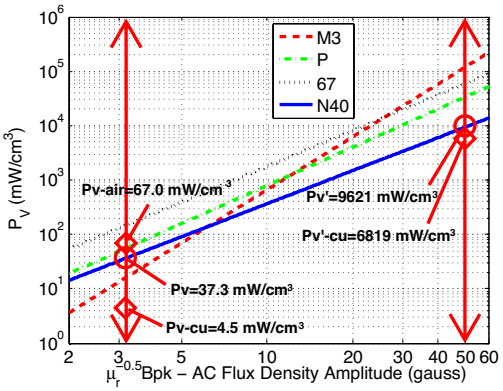

Fig. 9. The magnetic-core inductor after scaling design

loss $P_{V'-cu}$ of the magnetic-core inductor built with N40 material after scaling on the graph of P_V vs. $\mu_r^{-0.5}B_{pk}$ by (22), (24) and (27). In the example, $P'_V = 9621$ mW/cm^3 and $P'_{V-cu} = 6819$ mW/cm^3 are shown in Fig. 9. We can see that the core loss of N40 is the lowest among the materials. If we build a magnetic-core inductor with other materials with the same size after scaling, the inductor will have a lower quality factor and must have a bigger size to satisfy the design requirement for minimum quality factor; this confirms our conclusion that the magnetic-core inductor built with N40 has the smallest size.

E. Inductor Design with the Best Magnetic Material

Having satisfied quality factor Q_L and inductor size requirements, the inductor can be designed with the selected best magnetic material (N40). To provide a complete answer for the previous design example, we summarize the results of each step in Fig. 2:

1) We give the design requirements: $L = 200$ nH, $I_{pk} = 2$ A, $f_s = 30$ MHz, minimum $Q_L = 116$ and maximum size of $d_o = 12.7$ mm, $d_i = 6.3$ mm and $h = 6.3$ mm.
2) Given available magnetic materials (67, P, M3 and N40) and their Steinmetz parameters, we decide N40 is the best material for design.
3) Given the maximum size, estimate the highest Q_L of a magnetic-core inductor with N40 material (about $Q_L = 171$).
4) Given the minimum Q_L, estimate the scaling factor $\lambda = 0.17$ and the minimum size $d_o = 2.2$ mm, $d_i = 1.1$ mm and $h = 1.1$ mm calculated by (18).

5) We check the results in the third and fourth steps and see if they satisfy the design requirements.
6) If we prefer a core inductor with the highest Q_L as well as the maximum size, the inductor will have a a turns number $N = 4$ calculated by (6), an inductance $L = 199$ nH, the core size of $d_o = 12.7$ mm, $d_i = 6.3$ mm and $h = 6.3$ mm. Its quality factor Q_L has been estimated in Section III-C. If we prefer a cored inductor with the minimum size at the minimum allowed Q_L, the inductor will have a turns number $N' = 10$ calculated by (20) and the core size is $d_o = 2.2$ mm, $d_i = 1.1$ mm and $h = 1.1$ mm.

Compared to a coreless design, the magnetic-core inductor with N40 material will have 47% higher quality factor Q_L for the same maximum size or 83% size reduction for the same minimum quality factor.

IV. Experimental Verification

We carried several experiments to verify the design procedure illustrated in this paper. Firstly, we want to verify the design steps 2 and 3 in Fig. 2. That is, given available magnetic materials and design requirements (inductance L, current amplitude I_{pk}, and frequency f_s), we want to determine the best material to yield maximum quality factor Q_L for a given size, and estimate the highest Q_L that can be achieved at that size. Design parameters for the example application are repeated here: $d_o = 12.7$ mm, $d_i = 6.3$ mm, $h = 6.3$ mm, $L = 200$ nH, $I_{pk} = 2$ A, and $f_s = 30$ MHz. As predicted in our design procedure, N40 is the best material and the magnetic-core inductor with N40 has quality factor $Q_L = 171$. We designed and fabricated a magnetic-core inductor with copper foil and N40 core to satisfy the design specifications, and measured its inductance and quality factor by experimental methods in [2]. To make comparison with other designs, we fabricated a coreless inductor and magnetic-core inductors with 67, M3 and P materials and similar core sizes. The results are listed and compared in Table II. We can see the measurement results fit very well with the predicted values and the magnetic-core inductor with N40 material is the best design compared to others as we have predicted in our design procedure.

Secondly, we verified the design step 4 illustrated in Section III-D. That is, given L, I_{pk}, f_s and the minimum Q_L, determine the best material for design and estimate the minimum size achievable for that Q_L requirement. This experiment is much more difficult than the first one because limited availability of core sizes. If we design a magnetic-core inductor with N40 material which has the scaling factor $\lambda = 0.17$ as calculated in Section III-D, the inductor after scaling has 10 turns and dimensions $d'_o = 2.16$ mm, $d'_i = 1.07$ mm and $h' = 1.07$ mm. The winding of copper foil has a width of less than 0.34 mm. It is very hard to wind such a narrow copper foil on this tiny core by hand. The magnetic-core inductor with P material in Section III-D5 has a higher scaling factor λ and thus a larger core size after scaling. So we verified the design of P material instead of N40. The design parameters are repeated here: $L = 200$ nH, $I_{pk} = 0.5$ A, $f_s = 30$ MHz and $Q_L = 116$. The scaling factor $\lambda = 0.77$ calculated by (26) and shown in Table I. The core dimensions after scaling are $d'_o = 9.78$ mm, $d'_i = 4.85$ mm and $h' = 4.85$ mm. The available core with the closest size has dimensions OD$= 9.63$ mm, ID$= 4.66$ mm and Ht$= 3.21$ mm. We designed and fabricated a 3-turn magnetic-core inductor with P material and measured its inductance L and quality factor inductor Q_L. The results are shown in Table III. We can see the measurement results fit very well with the predicted value (for the actual size) and (26) is thus verified.

TABLE II
Comparison among coreless inductors and magnetic-core inductors designed at $I_{pk} = 2$ A and $f_s = 30$ MHz in different magnetic materials.

Material	N40	M3	P	67	Coreless
Suppliers	Ceramic Magnetics	National Magnetics Group	Ferronics	Fairrite	N/A
Permeability	15	12	40	40	1
Designations	T50252-5T	998	11-250-P	59670-00301	N/A
d_o (mm)	12.7	12.7	12.7	12.7	12.7
d_i (mm)	6.3	7.9	7.9	7.2	6.3
h (mm)	6.3	6.4	6.4	5.0	6.3
Turns Number N	4	5	3	3	14
Predicted L (nH)	199	180	219	203	173
Measured L (nH)	230	181	262	235	245
Predicted Q_L	171	74	81	39	116
Measured Q_L	167	65	87	45	96

TABLE III
Magnetic-core inductor designed at $L = 200$ nH, $I_{pk} = 0.5$ A and $f_s = 30$ MHz with the scaling factor $\lambda = 0.77$.

Material	Designation	N	Predicted L (nH)	Predicted Q_L
P	11-220-P	3	168	110
d'_o (mm)	d'_i (mm)	h' (mm)	Measured L (nH)	Measured Q_L
9.63	4.66	3.21	181	105

V. Conclusion

In this paper, we propose an inductor design procedure using low permeability magnetic materials. The design procedure is based on the use of Steinmetz parameters. With this procedure, different magnetic materials are compared fairly and fast, and both the quality factor Q_L and the size of a magnetic-core inductor can be predicted before the final design. We also compare a magnetic-core inductor design to a coreless inductor design in our design procedure. Some problems, such as optimization of magnetic-core inductors, are also investigated in this paper. The procedure and methods proposed in this paper can help to design a magnetic-core inductor with low-permeability rf core materials.

APPENDIX A
OPTIMIZATION OF MAGNETIC-CORE INDUCTORS

In Section III, different magnetic materials are compared and evaluated with the assumption that optimum magnetic-core inductors made in all these materials will have the same relative dimensions as the coreless design on which they are based. However, magnetic-core inductors may have their own relative optimum dimensions for the maximum quality factor Q_L or the minimum size for different materials, thus the methods proposed in Section III may not be a fair comparison. That is, we need to establish whether or not the best *shape* for an inductor changes significantly with scale or material characteristics.

As will be seen, the results are quite reasonable and the approaches of Section III lead to near optimum designs under a wide range of conditions. We consider one optimization case in this paper. We assume a magnetic-core toroidal inductor's d_o and h are restricted to be constant (e.g., as stipulated by the specification of a power electronics circuit), and we optimize d_i to get the maximum quality factor Q_L. In the optimization, make the assumption that core losses dominate and neglect copper loss. We do take into account the fact that the flux density inside the core is not uniform when calculating core loss.

The total core loss P_0 is calculated without the approximation of uniform flux. From (6),

$$B_{pk}(r) = \frac{\mu_0\mu_r N I_{pk}}{2\pi r} = \frac{I_{pk}}{r}\sqrt{\frac{\mu_0\mu_r L}{2\pi h \ln\left(\frac{d_o}{d_i}\right)}} \tag{28}$$

Where r specifies a radius from the center of the core ($\frac{d_i}{2} < r < \frac{d_o}{2}$).

$$\begin{aligned} P_0(d_i) &= \int_{\frac{d_i}{2}}^{\frac{d_o}{2}} P_V \mathrm{d}V = \int_{\frac{d_i}{2}}^{\frac{d_o}{2}} K B_{pk}(r)^\beta 2\pi r h \mathrm{d}r \\ &= 2\pi h K \left[I_{pk}\sqrt{\frac{\mu_0\mu_r L}{2\pi h \ln\left(\frac{d_o}{d_i}\right)}}\right]^\beta \int_{\frac{d_i}{2}}^{\frac{d_o}{2}} r^{1-\beta}\mathrm{d}r \end{aligned} \tag{29}$$

If $\beta \neq 2$,

$$P_0(d_i) = \frac{2\pi h K}{2-\beta}\left[I_{pk}\sqrt{\frac{\mu_0\mu_r L}{2\pi h \ln\left(\frac{d_o}{d_i}\right)}}\right]^\beta \left[\left(\frac{d_o}{2}\right)^{2-\beta} - \left(\frac{d_i}{2}\right)^{2-\beta}\right] \tag{30}$$

If $\beta = 2$,

$$P_0(d_i) = \mu_0\mu_r K L I_{pk}^2 \tag{31}$$

From (30) and (31), let $d_i = 0.5d_o$ and we normalize the total core loss $P_0(d_i)$ by the total loss P_0 at $d_i = 0.5d_o$. If $\beta \neq 2$,

$$\frac{P_0(d_i)}{P_0(0.5d_o)} = \left[\frac{\ln 2}{\ln\left(\frac{d_o}{d_i}\right)}\right]^{0.5\beta}\left[\frac{1-\left(\frac{d_i}{d_o}\right)^{2-\beta}}{1-0.5^{2-\beta}}\right] \tag{32}$$

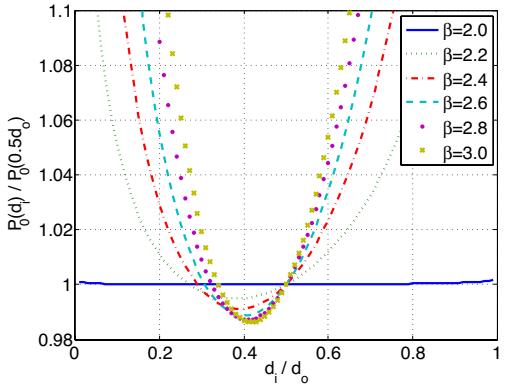

Fig. 10. Plot of core power loss dissipation in a rectangular cross-section toroidal core as a function of $\frac{d_i}{d_o}$, normalized to that with $\frac{d_i}{d_o} = 0.5$. Results are parameterized in Steinmetz parameter β. It can be seen that over a wide range of β, $\frac{d_i}{d_o} = 0.5$ is very close to the optimum, and that results are not highly sensitive to $\frac{d_o}{d_i}$.

If $\beta = 2$,

$$\frac{P_0(d_i)}{P_0(0.5d_o)} = 1 \tag{33}$$

In (32), $\frac{P_0(d_i)}{P_0(0.5d_o)}$ only depends on the ratio of $\frac{d_o}{d_i}$ and Steinmetz parameter β. We plot P_0 as a function of $\frac{d_o}{d_i}$ for different β in Fig. 10. From Fig. 10, we can see that the optimum d_i is around $0.4d_o$, with an exact value that depends β. When d_i varies between $0.22d_o$ and $0.64d_o$, the total core loss P is very flat and the deviation from the minimum core loss is less than 10%. We choose $d_i = 0.5d_o$ instead of $d_i = 0.4d_o$ for the following considerations: firstly, $d_i = 0.5d_o$ is a more typical dimension ratio for commercial magnetic cores (e.g., see Table II); secondly, as shown in [5], the error due to the assumption of average flux density is less than 10% if $d_i \leq 0.5d_o$. The error in assuming that the optimum inside diameter is $d_i = 0.5d_o$ is lower than 2% for a wide range of β values. So we can think $d_i = 0.5d_o$ as the nearly-optimum dimension for a wide range of magnetic materials. We can thus compare and evaluate different magnetic materials under the same dimensions and our assumption in Section III is correct. In Section III-D, we also use the same assumption to investigate (9), (11) and (17).

REFERENCES

[1] D. Perreault, J. Hu, J. Rivas, Y. Han, O. Leitermann, R. Pilawa-Podgurski, A. Sagneri, and C. Sullivan, "Opportunities and challenges in very high frequency power conversion," *24th Annu. IEEE Applied Power Electronics Conf. and Expo.*, pp. 1–14, Feb. 2009.

[2] Y. Han, G. Cheung, A. Li, C. Sullivan, and D. Perreault, "Evaluation of magnetic materials for very high frequency power applications," *39th IEEE Power Electronics Specialists Conf.*, pp. 4270–4276, Jun. 2008.

[3] R. Erickson and D. Maksimović, *Fundamentals of Power Electronics*, 2nd ed. Springer Science and Business Media Inc., 2001, ch. 14 and 15.

[4] C. Sullivan, W. Li, S. Prabhakaran, and S. Lu, "Design and fabrication of low-loss toroidal air-core inductors," *38th IEEE Power Electronics Specialists Conf.*, pp. 1757–1759, Jun. 2007.

[5] Y. Han, "Circuits and passive components for radio-frequency power conversion," Ph.D. dissertation, Massachusetts Institute of Technology, Feb. 2010.